Acta Geotechnica
https://doi.org/10.1007/s11440-018-0646-5

RESEARCH PAPER

Bearing capacity of pile groups under vertical eccentric load

Raffaele Di Laora[1] · Luca de Sanctis[2] · Stefano Aversa[2]

Received: 11 September 2017 / Accepted: 5 March 2018

Abstract
The paper deals with the problem of the bearing capacity of pile groups under vertical eccentric load. Widespread practice is to consider the achievement of the axial capacity on the outermost pile as the ultimate limit state of the pile group. However, this approach neglects the ductility of the foundation system and may be thereby overconservative. With the aim of proposing an alternative and more rational approach, a novel formulation for interaction diagrams based on theorems of limit analysis is presented and discussed. The methodology is applicable to the general case of groups of unevenly distributed, dissimilar piles. Piles' connections to the pile cap are modeled as either hinges or rigid-plastic internal fixities. An application example to a slender structure is also provided, showing that the proposed approach can lead to significant advantages over the traditional design.

Keywords Bearing capacity · Eccentric loading · Limit analysis · Pile groups

List of symbols

α	Adhesion factor
α_M	Inclination of the applied moment vector
γ_b, γ_s	Partial resistance factors for pile base and shaft capacity
γ_{st}	Partial factor for shaft capacity in tension
γ_{su}	Partial factor for undrained shear strength
δ	Coefficient depending on number of piles
$\delta\theta$	Increment of rotation
δW_i, δW_k	Increments of work done by internal forces
δE_i, δE_k	Increments of work done by external forces
η	Efficiency of a pile group
ξ_3	Correlation factor to derive characteristic value
ξ_j	Coordinate of the j-th pile in the reference system (ξ, η)
σ_{VL}	Total overburden stress at depth L
A_b	Base area of the block containing the piles
A_s	Side area of the block containing the piles
B	Distance between two external piles of a row
c	Abscissa of the center of the row
d	Pile diameter
L	Pile length
M	External moment vector
M_0	Moment capacity of the pile group under zero axial loading
M_u, M_{ui}, M_{uk}	Moment capacities of the pile group
M_{ux}, M_{uy}	Moment capacities along x- and y-axes in the 3D domain
m	Number of alignments of piles parallel to external moment vector M
m_{yc}, m_{yt}	Dimensionless yielding bending moments
M_{yc}, M_{yt}	Yielding bending moments
N_c	Bearing capacity factor
N_u	Axial capacity of the single pile in compression
N_{uj}	Axial capacity in compression of the j-th pile
n	Number of piles in a row
p	Number of piles in a group
p_k	Unit base resistance
P_k	Characteristic value of pile base resistance
Q	External axial capacity
Q_i, Q_j	Axial loads on piles i an j
Q_0	Axial capacity of the pile group
Q_u, Q_{ui}, Q_{uk}	Axial capacity of the pile group
S_k	Characteristic value of pile shaft resistance
S_u	Axial capacity of the single pile in uplift
S_{uj}	Axial capacity in uplift of the j-th pile

✉ Raffaele Di Laora
raffaele.dilaora@unicampania.it

[1] Università della Campania "Luigi Vanvitelli", Aversa, CE, Italy

[2] Università di Napoli Parthenope, Napoli, Italy

Published online: 31 March 2018

s	Pile spacing
s_k	Unit shaft resistance
s_u	Soil undrained shear strength
x_j	Abscissa of the j-th pile
y_j	Ordinate of the j-th pile

1 Introduction

Axially loaded piles should be designed to provide adequate strength against a bearing capacity failure. In many engineering problems, pile groups are loaded eccentrically, that is, the external load is not applied on the center of the axial capacities of the individual piles, as shown in Fig. 1.

Under centered load, the difference between the axial capacity of a group of piles and that of the single pile, N_u, multiplied by the number of piles, p, has been traditionally characterized by an efficiency factor, η, depending on both pile and soil type [14]:

$$Q_u = \eta \cdot p \cdot N_u \tag{1}$$

The proper value of the efficiency may be selected on the basis of the available experimental evidence [2, 3, 6, 7, 23, 32, 34, 35]. The above concept applies to the failure mode corresponding to individual pile capacities. However, collapse of pile groups may occur also by failure of the overall block of soil containing the piles [11, 31]. Fleming et al. [11] claim that block failure for granular soils occurs when the base area is much smaller than the side area ($A_b/A_s < 1$). As a result, group of closely spaced long piles are more likely to fail as a block than groups of short piles at relatively large spacing. For fine-grained soils in undrained conditions, block failure is even more likely to occur. Experiments carried out by many researchers (e.g., [6, 7]) suggested that groups with piles at spacing smaller than a critical value (say 2–4 times the pile diameter d) fail as 'blocks'. Independent calculation of both modes of failure should be therefore carried out, and the bearing capacity of the pile group taken as the lesser of the two capacities.

In case of eccentric loads (Fig. 1), the most widespread approach is that of considering the achievement of the axial capacity (in compression or in uplift) on the outermost pile as the ultimate limit state of the pile group, as recommended, for example, by AASHTO Bridge Design Specifications [1]. The implication in design of such an assumption is described in Fig. 2, referring to a 1×4 group of identical piles connected by a rigid cap and loaded by a vertical force acting along the axis of the first pile. For the sake of simplicity, the four piles are considered as linear elastic, perfectly plastic independent springs, with equal strength in compression (N_u) and in uplift ($-S_u$). Under these hypotheses, the load distribution varies linearly with the distance along the cap until the achievement of the axial capacity on the first pile. According to the common approach, the axial capacity of the pile group would be $Q_u = 10/7N_u$. However, the achievement of the axial capacity on pile 1 does not represent a failure condition for the whole group and can be viewed just as the onset of yielding. At this point, the pile group is still capable to carry a further increase in the external load taking advantage from the ductility of the system. For example, an external load $Q_u = 2N_u$ (that is 40% larger than $10/7N_u$) might be equilibrated by a load distribution where piles from 1 to 3 achieve the axial capacity in compression and pile 4 that in uplift. Such a load distribution does not violate the failure criterion adopted for the piles and, thus, is a lower bound solution of the problem under examination. Therefore, the common approach is unduly conservative.

Attention has been placed in the past on the assessment of interaction diagrams (Q_u, M_u) of pile groups on an experimental basis. Research works on this subject include reduced scale tests on groups of steel piles loaded by a vertical and eccentric load and resting on both sand

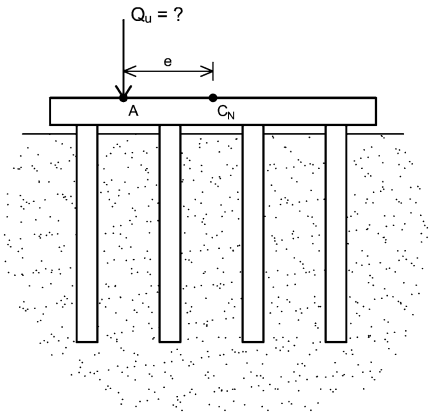

Fig. 1 Problem under investigation: bearing capacity of a pile group under vertical eccentric load

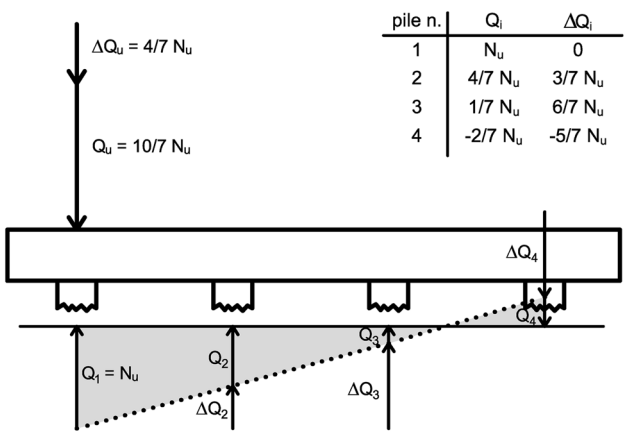

Fig. 2 Conservatism of the conventional approach

[15, 18, 20] and saturated clay [17, 19, 27]. Semiempirical interaction relationship between the axial and moment capacity based on the above experimental evidence is also available. For groups of piles embedded in sand, Meyerhof et al. [20] suggest to adopt the following expressions:

$$\left(\frac{Q_u}{Q_0}-0.4\right)^2+\frac{M_u}{M_0}=1 \quad \text{for } \frac{Q_u}{Q_0}\geq 0.4$$
$$\frac{Q_u}{Q_0}=\frac{2}{3}\left(\frac{M_u}{M_0}-0.4\right) \quad \text{for } \frac{Q_u}{Q_0}\leq 0.4 \qquad (2a, b)$$

where Q_0 and M_0 represent the axial capacity of the pile group with zero moment and the moment capacity with zero axial load, respectively.

For groups of piles embedded in clayey soils, Meyerhof and Yalcin [19] propose a unique parabolic relationship:

$$\left(\frac{Q_u}{Q_0}\right)^2+\frac{M_u}{M_0}=1 \qquad (3)$$

However, the application in practice of Eqs. (2) and (3) is not immediate, because of the inherent difficulties associated with the evaluation of the moment capacity with zero axial load. In addition, the available evidence is limited to reduced scale pile groups resting on homogeneous soils.

Moving to the design perspective, recent codes seem to be fully aware of the conservatism associated with the common approach. For example, Eurocode 7 [5] claims that 'for piles supporting a stiff structure, a failure will occur only if a significant number of piles fail together', outlining that 'a failure mode involving only one pile need not be considered'. Similarly, according to the Italian building code [22], an axially loaded pile group achieves an ultimate limit state only when 'the piled foundation fails as a whole'. Nevertheless, such statements are not supported by any indication on the calculation method to be applied to predict the bearing capacity of the pile group. An example on how to perform a plastic calculation alternative to the conventional approach can be found in [10] and is referred to as 'fully plastic calculation'. In this application, a discrete number of ultimate strength points is evaluated by imposing that piles achieve together the axial capacity in compression or in uplift. At the same time, FEMA 750 claims that 'the plastic analysis approach is likely to overestimate the strength that a multi-pile group is capable of developing'; as a result, 'many engineer would prefer the conventional approach', based on a linear relationship between the axial and moment capacities. Furthermore, the calculation example supplied by FEMA does not shed any light on the plastic mechanism occurring at failure.

Although codes seem to recognize the conservatism of the conventional approach, there is still lack of understanding about the mechanism governing the failure of a pile group under vertical and eccentric load, even from a theoretical standpoint.

This work is aimed at filling this gap, by providing a theoretical framework in which the beneficial role played by the ductility of the foundation system is explicitly taken into account. In this respect, a novel closed-form exact formulation for moment-axial force interaction diagrams of groups of unevenly distributed, dissimilar piles hinged at the top is presented and discussed. In addition, when the connection of the pile top to the cap is restrained against rotation, an accurate lower bound solution is supplied.

2 Interaction diagrams from limit analysis theorems: exact solution

2.1 General

In order to determine the collapse load of a pile group under vertical eccentric loads, the following assumptions are made: (a) piles are modeled as rigid-plastic independent uniaxial elements, characterized by two yielding loads, one in compression (N_u) and one ($-S_u$) in uplift, intended as the capacities of the single pile within the group; (b) piles' heads are connected through a rigid cap having infinite strength; (c) the connections of the piles to the cap are modeled as hinges, i.e., internal forces on piles consist only of axial loads (pinned piles).

The assumption of rigid cap (b) is a reasonable hypothesis in many engineering problems, since the evaluation of the ultimate capacity of a pile group is generally of concern for small piled rafts [9, 25, 26]. With reference to (c), the contribution of the yielding moments to the overall failure domain of the pile group is usually negligible in case of slender piles; by contrast, it may be relevant for squatty piles, because yielding moments are proportional to d^3, with d the pile diameter.

In principle, the expression of the interaction diagram can be derived by solving directly the problem of a rigid cap supported on rigid-plastic uniaxial elements, by imposing equilibrium conditions and compatibility of vertical displacements at the piles' heads for cap rotation about an arbitrary point. An alternative, more elegant and conceptually more effective approach is based on theorems of limit analysis. Noticeably, the basic hypothesis of associative flow rule is implicitly satisfied, because plastic displacements of piles have the same direction of yielding loads. The upper bound theorem states that: if there is a set of external loads and a compatible collapse mechanism such that the increment of work of the external loads equals the increment of energy dissipated by internal stresses, the collapse occurs and the set of external loads represent an upper bound to the 'real' solution of the collapse problem.

Since this theorem considers the kinematics of the collapse mechanism, it is also defined as kinematic theorem. The lower bound theorem states that: if there is a set of external loads in equilibrium with internal stresses that do not exceed the yield stress in any point, the collapse does not occur and the external loads represent a lower bound to the 'real' collapse load. Since this theorem refers only to static equilibrium conditions, it is defined also as static theorem.

2.2 Row of equally spaced, identical piles

Reference is made to a row of equally spaced, identical piles, as shown in Fig. 3. The origin of the x-axis is taken as coincident with the center of the row. In the realm of the upper bound theorem of limit analysis, Fig. 3a shows a plastic mechanism where the capped pile group displaces by rotation about point C located between pile $(i-1)$ and pile (i). The external collapse load corresponding to such a mechanism can be defined as (Q_{ui}, M_{ui}); in this respect, the variable 'i' identifies both pile i within the row and the plastic mechanism characterized by a counterclockwise increment of rotation about a point between pile $(i-1)$ and pile i. Since all piles behave like rigid-perfectly plastic elements, the axial load mobilized by any increment of rotation, $\delta\theta$, is equal to N_u or $(-S_u)$. Taking into account the sign convention shown in Fig. 3, the increment of work done by external forces (Q_{ui}, M_{ui}) is given by $(i = 1, \ldots, n)$:

$$\delta E_i = M_{ui}\delta\theta + Q_{ui}c\delta\theta \tag{4}$$

while the increment of work done by internal forces is:

$$\delta W_i = -\sum_{j=1}^{i-1}(x_j - c)\delta\theta N_u + \sum_{j=i}^{n}(x_j - c)\delta\theta S_u \tag{5}$$

where c is the abscissa of point C and n is the number of piles.

It is easy to verify that Eq. (5) leads to:

$$\delta W_i = \delta\theta\frac{s}{2}(N_u + S_u)(i-1)(n-i+1) + \delta\theta c[N_u(i-1) - S_u(n-i+1)] \tag{6}$$

By equating $\delta W_i = \delta E_i$, the upper bound solution is found $(i = 1,\ldots, n)$:

$$\begin{cases} Q_{ui} = N_u(i-1) - S_u(n-i+1) \\ M_{ui} = \dfrac{s}{2}(N_u + S_u)(i-1)(n-i+1) \end{cases} \tag{7}$$

Noticeably, the coordinates (Q_{ui}, M_{ui}) do not depend on the exact position of the center of rotation between piles $(i-1)$ and i.

For a clockwise increment of rotation between pile $(k-1)$ and (k), the increment of work done by external forces (Q_{uk}, M_{uk}) is $(k = 1, \ldots, n)$:

$$\delta E_k = M_{uk}\delta\theta + Q_{uk}c\delta\theta \tag{8}$$

while the increment done by internal forces is

$$\delta W_k = \sum_{j=1}^{k-1}(x_j - c)\delta\theta S_u - \sum_{j=k}^{n}(x_j - c)\delta\theta N_u \tag{9}$$

The latter quantity can be cast in the form:

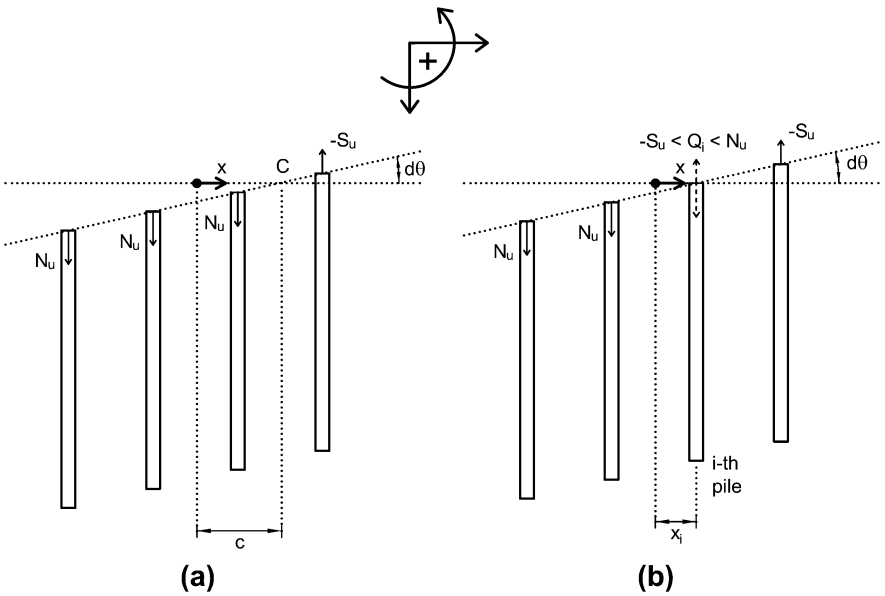

Fig. 3 Collapse mechanism for a row of equally spaced, identical piles: **a** rotation about a point between two piles; **b** rotation about the head of a pile

$$\delta W_k = -\delta\theta\frac{s}{2}(N_u + S_u)(i-1)(n-i+1) + \delta\theta c[-(k-1)S_u + (n-k+1)N_u] \quad (10)$$

As before, the variable k identifies both pile k-th within the row and the plastic mechanism characterized by a clockwise increment of rotation about a point between pile $(k-1)$ and k.

By equating $\delta W_k = \delta E_k$, the following expression is found:

$$\begin{cases} Q_{u(k+n)} = -(k-1)S_u + (n-k+1)N_u \\ M_{u(k+n)} = -\dfrac{s}{2}(N_u + S_u)(k-1)(n-k+1) \end{cases} \quad (11)$$

It is easy to verify that Eq. (11) can be obtained from Eq. (7) by substituting N_u with $(-S_u)$ and vice versa. Equation (11) is also equivalent to ($i = n + 1, \ldots, 2n$):

$$\begin{cases} Q_{ui} = -(i-n-1)S_u + (2n-i+1)N_u \\ M_{ui} = -\dfrac{s}{2}(N_u + S_u)(i-n-1)(2n-i+1) \end{cases} \quad (12)$$

Noticeably, Eq. (11) can be derived from Eq. (12) by replacing $(i-n)$ with k. Equations (7) and (11), or (7) and (12), define a set of $2n$ upper bound solutions corresponding to cap rotations about any point located between two consecutive piles or on the left of pile 1, the latter condition representing pure compression or pure traction. External loads (Q_{ui}, M_{ui}) with $i = (1,\ldots 2n)$ define a polygonal line in (Q_u, M_u) plane, obtained by drawing the conjunction lines between consecutive points.

An application of Eqs. (7) and (11) is depicted in Fig. 4, referring to the pile layout shown in Fig. 3 and $S_u = 3/4N_u$.

The number of conjunction lines between consecutive points is $2n$. The corresponding equations in (Q_u, M_u) plane can be written as:

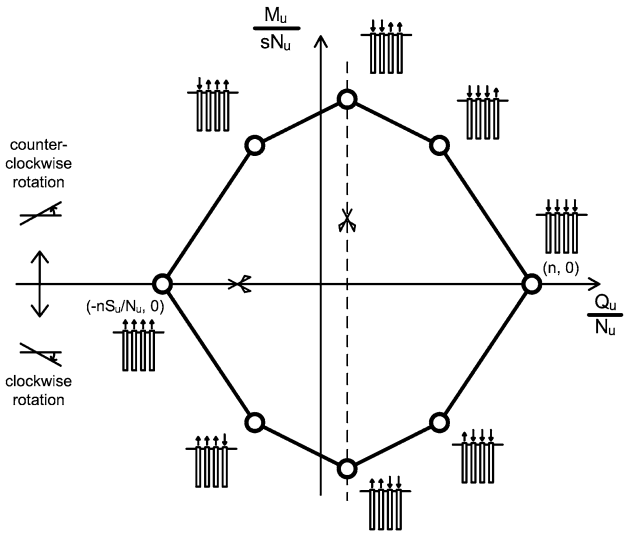

Fig. 4 Interaction diagram for a row of 4 identical, equally spaced piles

$$M_u = M_{ui} + (Q_u - Q_{ui})\frac{s}{2}(n-2i+1)\,i \quad = 1,\ldots,2n \quad (13)$$

It is easy to verify that the conjunction lines between any two consecutive points also represent subsets of upper bound solutions. To prove this, Fig. 3b shows a mechanism of plastic collapse consisting of a rotation about the head of pile i-th. Proceeding as before, for a counterclockwise increment of rotation we have ($i = 1,\ldots, n$):

$$\delta E_i = M_u\delta\theta + Q_u x_i\delta\theta \quad (14)$$

$$\delta W_i = -\sum_{j=1}^{i}(x_j - x_i)\delta\theta N_u + \sum_{j=i+1}^{n}(x_j - x_i)\delta\theta S_u \quad (15)$$

where

$$Q_u = (i-1)N_u + Q_i - (n-i)S_u \quad -S_u \le Q_i \le N_u \quad (16)$$

The increment of work done by internal forces can be written as:

$$\delta W_i = M_{ui}\delta\theta - \frac{s}{2}(n-2i+1)Q_{ui}\delta\theta \quad (17)$$

Equating the increments of work done by internal and external forces leads to:

$$M_u = M_{ui} + \frac{s}{2}(n-2i+1)(Q - Q_{ui}) \quad (18)$$

For a clockwise rotation, the same solution is recovered. Equation (18) is identical to Eq. (13) and thus corresponds to the conjunction lines between consecutive vertexes. Note that the domain is characterized by two axes of symmetry, since the origin of the coordinate system is taken as the center of the row. The vertical axis of symmetry coincides with the y-axis when the axial capacity in compression is equal to that in uplift.

It may be convenient to write Eqs. (7) and (11) in the following dimensionless form:

$$\begin{cases} \dfrac{Q_{ui}}{N_u} = i - 1 - \dfrac{S_u}{N_u}(n-i+1) \\ \dfrac{M_{ui}}{sN_u} = \dfrac{1}{2}\left(1 + \dfrac{S_u}{N_u}\right)(i-1)(n-i+1) \end{cases} \quad i = 1,\ldots,n \quad (19)$$

$$\begin{cases} \dfrac{Q_{u(k+n)}}{N_u} = -\dfrac{S_u}{N_u}(k-1) + (n-k+1) \\ \dfrac{M_{u(k+n)}}{sN_u} = -\dfrac{1}{2}\left(1 + \dfrac{S_u}{N_u}\right)(k-1)(n-k+1) \end{cases} \quad k = 1,\ldots,n \quad (20)$$

The maximum and minimum axial dimensionless loads, occurring at zero moment, are:

$$\left(\frac{Q_u}{N_u}\right)_{\max} = n$$
$$\left(\frac{Q_u}{N_u}\right)_{\min} = -n\frac{S_u}{N_u} \tag{21}$$

It is straightforward to demonstrate that the maximum dimensionless moment is:

$$\left|\frac{M_u}{sN_u}\right|_{\max} = \left(1+\frac{S_u}{N_u}\right)\frac{n^2-\delta}{8} \tag{22}$$

with $\delta = 0$ if n is even and 1 if n is odd.

It is worthy of note that a load distribution satisfying Eqs. (7), (11) and (13) does not violate the failure criterion and, hence, represent also a lower bound solution. Therefore, an interaction diagram like that represented in Fig. 4 is an exact solution, and there is no point in seeking load distributions other than those obtained by the plastic mechanisms defined in Fig. 3.

Based on the above results, the following main conclusions can be drawn:

a. A pile group subjected to vertical and eccentric load will fail by a cap rotation about the head of a pile, as shown in Fig. 3b; under this collapse mechanism, all piles within the group achieve their ultimate axial capacity in compression or in uplift, with the exception of the pile corresponding to the center of rotation;
b. The vertexes of the interaction diagram represent singularities; when the external load on the capped pile group corresponds to a vertex, the plastic mechanism is indeterminate, and failure occurs by a cap rotation about an indefinite point in between two consecutive piles, as shown in Fig. 3a; under this circumstance, all piles achieve their axial capacity.

2.3 Groups of identical piles

A group of equally spaced, identical piles subjected to an external moment vector, M, inclined by α_M with respect to y-axis, is first examined (Fig. 5). Since piles are supposed identical, the center of the capacities in compression, C_N, corresponds to that in uplift, C_T. For the sake of simplicity, the origin of the reference system (X, Y) is taken coincident with C_N (or C_T). A new reference system (ξ, η) can be defined, with the η-axis coincident with the direction of the resultant moment vector M, as shown in Fig. 5.

The interaction diagram consists of $2p$ points, where p is the number of piles within the group. Proceeding as before, the coordinates of the vertexes can be written as:

$$\begin{cases} Q_{ui} = (i-1)N_u - (p-i+1)S_u \\ M_{ui} = -N_u\sum_{j=1}^{i-1}\xi_j + S_u\sum_{j=i}^{p}\xi_j \end{cases} \quad i = 1,\ldots,p \tag{23}$$

and

$$\begin{cases} Q_{uk} = -(k-1)N_u + (p-i+1)S_u \\ M_{uk} = S_u\sum_{j=1}^{i-1}\xi_j - N_u\sum_{j=k}^{p}\xi_j \end{cases} \quad k = 1,\ldots,p \tag{24}$$

where

$$\xi_j = x_j\cos\alpha_M - y_j\sin\alpha_M \tag{25}$$

It is easy to verify that the conjunction lines between these points still represent an exact solution. Note that in the particular case of a rectangular group of identical piles with constant spacing s along both x and y direction and $\alpha_M = 0$, the conjunction lines between two consecutive points are described by the same equations as for the row of piles:

$$M_u = M_{ui} + (Q_u - Q_{ui})\frac{s}{2}(p-2i+1) \text{ for } \quad i = 1,\ldots,2p \tag{26}$$

Figure 5 also illustrates the interaction diagrams of the pile group examined herein for different values of α_M. Generally, any alignment parallel to the resultant moment vector does not catch more than one pile. However, there might be alignments passing through two or more piles; in this case, the number of vertexes reduces from $2p$ to $2m$, where m is the total number of different alignments parallel to vector M including at least one pile.

The interaction domain is always characterized by two axes of symmetry, whatever be the inclination of vector M, provided that the origin of the reference system coincides with the center of the pile capacities in compression (or in uplift).

The failure locus of the pile group shown in Fig. 5 is plotted in Fig. 6 in the (Q_u, M_{ux}, M_{uy}) space, in line with what is commonly done in the literature for failure envelopes of shallow foundations [4, 12, 13, 21, 24, 28]. Due to symmetry, only a quarter of the overall domain is represented. The cross sections of the failure locus at constant Q_u are also plotted in Fig. 6. It can be noticed that the 3D failure locus is not convex, making complicated the comparison with the applied load. Thus, taking also into account the inherent difficulty associated with the construction of the 3D domain, a comparison in the (Q_u, M_u) plane along the direction of the applied moment vector will be preferable form a practical viewpoint.

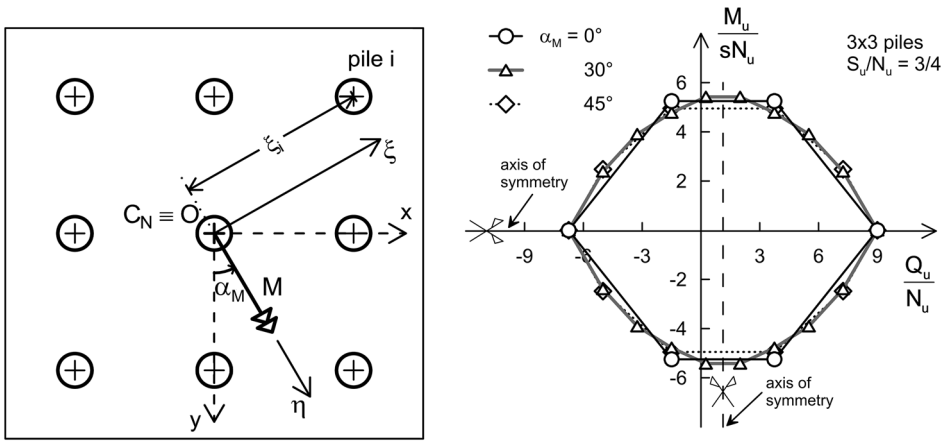

Fig. 5 Interaction diagram for an inclined moment vector

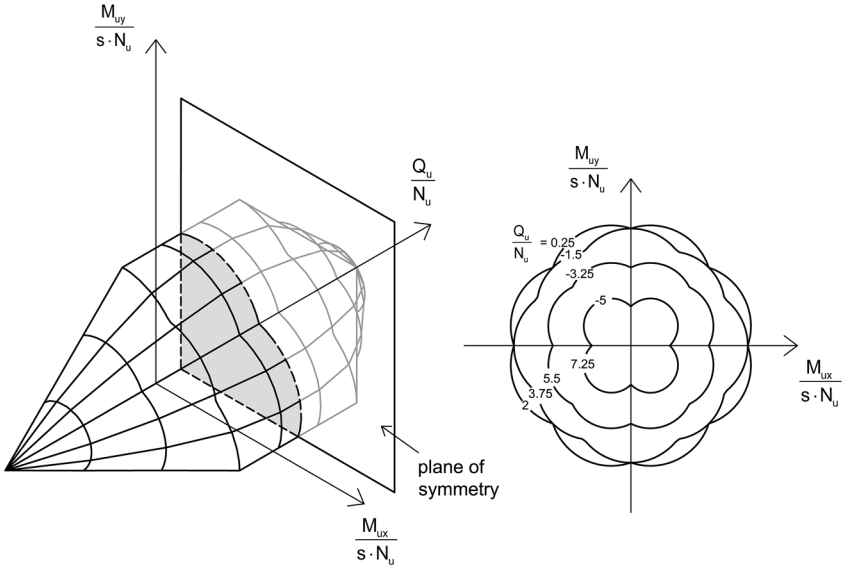

Fig. 6 Interaction diagram in the (Q_u, M_{ux}, M_{uy}) space

2.4 Groups of unevenly distributed, dissimilar piles

The above approach can be easily extended to the general case of a group of unevenly distributed, dissimilar piles:

$$\begin{cases} Q_{ui} = \sum_{j=1}^{i-1} N_{uj} - \sum_{j=i}^{p} S_{uj} \\ M_{ui} = -\sum_{j=1}^{i-1} N_{uj}\xi_j + \sum_{j=i}^{p} S_{uj}\xi_j \end{cases} \quad i = 1,\ldots,p \tag{27}$$

$$\begin{cases} Q_{u(k+p)} = \sum_{j=k}^{p} N_{uj} - \sum_{j=1}^{k-1} S_{uj} \\ M_{u(k+p)} = \sum_{j=1}^{k-1} S_{uj}\xi_j - \sum_{j=k}^{p} N_{uj}\xi_j \end{cases} \quad k = 1,\ldots,p \tag{28}$$

An application of Eqs. (27) and (28) to a row of 4 piles, each of them having different failure load both in compression and in tension, is illustrated in Fig. 7. The domain is characterized by a polar symmetry that does not coincide with the origin of the reference system; moreover, the maximum and minimum values of the ultimate axial load are associated with a nonzero ultimate moment.

3 Effect of the yielding moments at the piles' head: approximate solution

The connections of the piles to the cap can be idealized as rigid-plastic internal fixities, to take advantage from the additional strength supplied by yielding moments developing at the piles' heads. In this case, applying the theorems of limit analysis leads to:

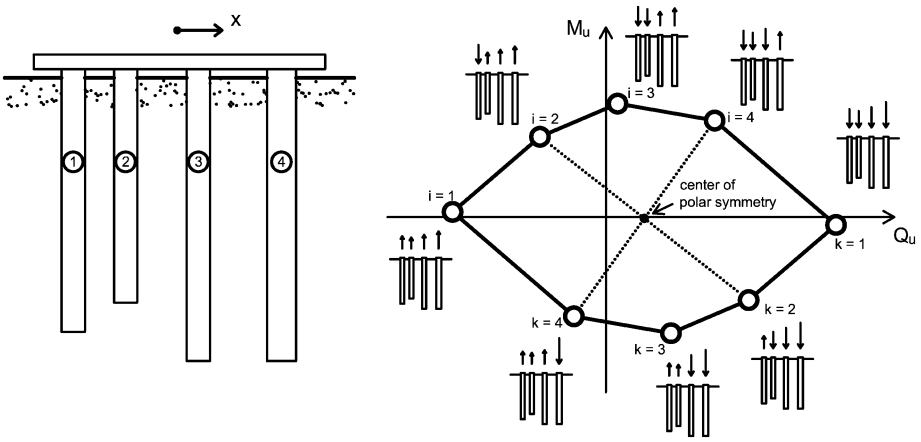

Fig. 7 Interaction diagram for a group of unevenly distributed dissimilar piles

$$\begin{cases} \dfrac{Q_{ui}}{N_u} = i - 1 - \dfrac{S_u}{N_u}(n - i + 1) \\ \dfrac{M_{ui}}{sN_u} = \dfrac{1}{2}\left(1 + \dfrac{S_u}{N_u}\right)(i-1)(n-i+1) \\ \quad + (n - i + 1)m_{yt} + (i-1)m_{yc} \end{cases} \quad i = 1, \ldots, n+1 \tag{29}$$

$$\begin{cases} \dfrac{Q_{u(k+n+1)}}{N_u} = -\dfrac{S_u}{N_u}(k-1) + (n-k+1) \\ \dfrac{M_{u(k+n+1)}}{sN_u} = -\dfrac{1}{2}\left(1 + \dfrac{S_u}{N_u}\right)(k-1) \\ (n-k+1) - (n-k+1)m_{yt} - (k-1)m_{yc} \end{cases} \quad \begin{array}{l} k = 1, \ldots, \\ n+1 \end{array} \tag{30}$$

where

$$\begin{aligned} m_{yt} &= \frac{M_{yt}}{sN_u} \\ m_{yc} &= \frac{M_{yc}}{sN_u} \end{aligned} \tag{31a, b}$$

and M_{yt} and M_{yc} yielding bending moments corresponding to $(-S_u)$ and N_u, respectively. In this case, the domain has $(2n + 2)$ vertexes. Noticeably, for $m_{yt} = m_{yc} = 0$ Eqs. (29) and (30) simplify to Eqs. (19) and (20).

For a group of unevenly distributed, dissimilar piles, the coordinates of the vertexes become:

$$\begin{cases} Q_{ui} = \sum_{j=1}^{i-1} N_{uj} - \sum_{j=i}^{p} S_{uj} \\ M_{ui} = \sum_{j=1}^{i-1} \left(M_{ycj} - N_{uj}\xi_j\right) \\ \quad + \sum_{j=i}^{p} \left(M_{ytj} + S_{uj}\xi_j\right) \end{cases} \quad i = 1, \ldots, p+1 \tag{32a, b}$$

$$\begin{cases} Q_{u(k+p+1)} = -\sum_{j=1}^{k-1} S_{uj} + \sum_{j=k}^{p} N_{uj} \\ M_{u(k+p+1)} = \sum_{j=1}^{k-1} \left(S_{uj}\xi_j - M_{ytj}\right) \\ \quad - \sum_{j=k}^{p} \left(M_{ycj} + N_{uj}\xi_j\right) \end{cases} \quad k = 1, \ldots, p+1 \tag{33a, b}$$

While the above points represent an exact solution, the conjunction lines between consecutive points deserve special attention. Connecting with a straight line points i and $(i + 1)$ implies assuming a linear relationship between the yielding moment of pile i and the axial load Q_i in the range $(-S_{ui}; N_{ui})$. Although this assumption does not correspond to reality, owing to the convexity of the flexural domain of the section, straight lines represent lower bound solutions. Further, considering that for any conjunction line the linear approximation is made only for the moment capacity of one pile, such lower bound solution will be very close to the rigorous, more complicated, exact domain, and is therefore suitable for engineering applications.

Figure 8 shows the interaction diagrams for different values of the yielding moment in compression, by taking a constant value of the ratio m_{yc}/m_{yt}. Due to different sectional moment capacities in compression and tension, the symmetry with respect to a vertical axis is lost.

4 Use of the results for design purposes

This section provides a comparison between the proposed and the conventional approach, the latter being applied with or without considering the interaction among piles. Figure 9 depicts interaction diagrams for 3^2 and 7^2 pile

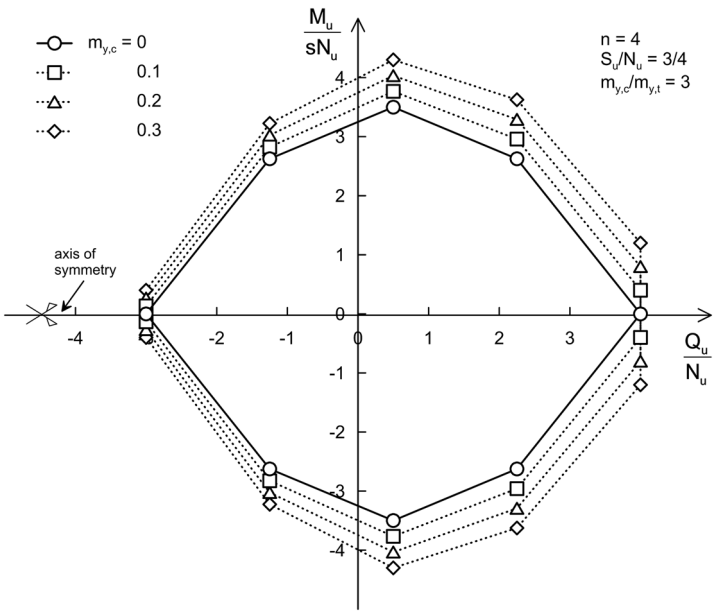

Fig. 8 Effect of the sectional flexural capacity on the interaction diagram for a row of 4 identical, equally spaced piles

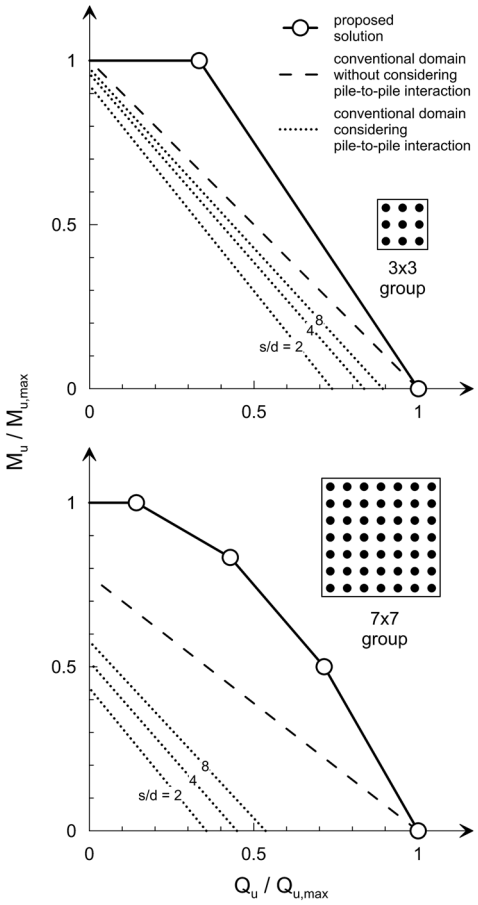

Fig. 9 Comparison between the proposed and the traditional approach. Pile-to-pile interaction is considered through the interaction coefficient supplied by Dobry and Gazetas [8]

groups assuming for the sake of simplicity equal strength in compression and uplift (i.e., $S_u/N_u = 1$). This is a reasonable assumption in the case of slender piles in soft clay, where the failure mechanism involving pile tip furnishes a negligible contribution to the overall capacity.

For the conventional interaction diagram without interaction effects, the following equations can be written:

$$\begin{cases} N_u = \dfrac{Q_u}{p} + \dfrac{M_u}{\sum\limits_{i=1}^{p} x_i^2}\dfrac{B}{2} \\ -S_u = \dfrac{Q_u}{p} - \dfrac{M_u}{\sum\limits_{i=1}^{p} x_i^2}\dfrac{B}{2} \end{cases} \tag{34}$$

where B is the distance between the two external piles.

Since piles are equally spaced, Eq. (34) simplifies to:

$$\begin{cases} M_u = -\dfrac{s(n+1)}{6}(Q_u - nN_u) \\ M_u = \dfrac{s(n+1)}{6}(Q_u + nS_u) \end{cases} \tag{35}$$

The maximum moment is the ordinate of the intersection point between the two lines represented by Eq. (35):

$$M_{u\max 1} = \frac{s}{6}(n+1)\frac{nS_u + nN_u}{2} \tag{36}$$

On the other hand, the maximum moment of the interaction domain based on limit analysis can be obtained from Eq. (22):

$$M_{u\max 2} = \frac{s}{4}\frac{n^2 - \delta}{n}\frac{nS_u + nN_u}{2} \tag{37}$$

It is immediate to recognize that M_{umax2} is always larger than M_{umax1}, and hence, the proposed interaction diagram is less conservative than the conventional domain for any eccentricity of the external load.

In addition, considering pile-to-pile interaction leads to a contraction of the conventional domain because of the occurrence of edge effects, thereby resulting in overconservative design especially for small pile spacing.

From comparison illustrated in Fig. 9, it is evident that using the proposed interaction diagram leads to undeniable advantages in the evaluation of the bearing capacity of a pile group under vertical eccentric load, particularly in the case of large eccentricity.

5 Application to a case study

An application to a case study is presented herein to highlight the potential beneficial effect of the proposed approach. The case examined in this work is a wind farm with 23 turbines constructed in South Italy. Each wind turbine is 95 m high and is founded on a circular raft enhanced with 16 cast in situ bored piles 22 m long and 0.8 m in diameter. The total pile length, nL, which may be considered roughly proportional to the cost of the piles, is 8096 m. Figure 10 illustrates a plan view and a cross section of a wind turbine. Also shown in this figure is the typical subsoil profile encountered at the site under examination, consisting essentially of a deep layer of overconsolidated, inorganic silty clay of high plasticity up to a depth of about 15 m, underlain by a very stiff, inorganic clay layer of medium plasticity and covered by a layer of silty sand; the ground water table was found at 2.0 m from the ground level. Site investigations included boreholes, standard penetration tests and down-hole tests, while laboratory tests consisted primarily of unconsolidated and undrained triaxial tests. Undrained shear strength, s_u, was therefore estimated as 196 kPa in the intermediate layer and 232 kPa in the lower stiff clay.

Unit base and shaft strength were evaluated in undrained conditions in terms of total stress through the following equations:

$$p_k = \sigma_{VL} + N_c s_u \tag{38}$$

$$s_k = \alpha s_u \tag{39}$$

where σ_{VL} is the total overburden stress at the depth L of the pile base, $N_c = 9$ [16, 29], and α is a coefficient depending on the pile installation technique and the undrained shear strength. For replacement piles and $s_u \geq 70$ kPa, α can be taken equal to 0.35 [33]. Finally, the design value of the single pile capacity in compression was evaluated through the following expression [5]:

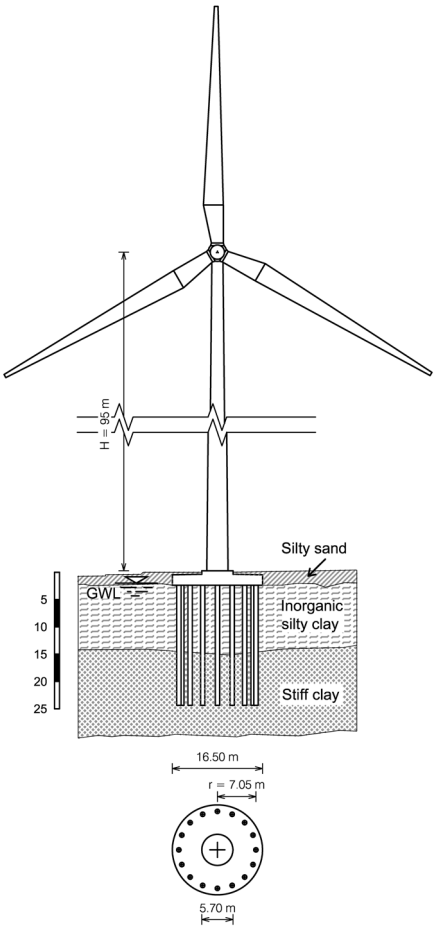

Fig. 10 Plan view and cross section of the piled foundation of the wind turbine under examination

$$N_u = \frac{P_k}{\gamma_b} + \frac{S_k}{\gamma_s} = \frac{\pi d^2}{4\xi_3\gamma_b}\left(\sigma_{\mathrm{VL}} + \frac{N_c s_u}{\gamma_{su}}\right) + \frac{\pi d}{\xi_3\gamma_s\gamma_{su}}\int_0^L s_k \mathrm{d}z \tag{40}$$

where γ_b and γ_s are partial resistance factors for pile base and shaft capacities, γ_{su} is the partial factor for undrained shear strength, and ξ_3 is the correlation factor to derive characteristic value from ground test results. In the short term, the uplift capacity of a bored pile in clay is likely to be equal to the shaft capacity in compression [11, 30]; hence,

$$S_u = \frac{S_k}{\gamma_{st}} = \frac{\pi d}{\xi_3\gamma_{st}\gamma_{su}}\int_0^L s_k \mathrm{d}z \tag{41}$$

where γ_{st} is the partial factor of the shaft capacity in uplift. Design approach 2 of Eurocode 7 and partial factors from the Italian national annex ($\gamma_b = 1.35$, $\gamma_s = 1.15$, $\gamma_{st} = 1.25$, $\gamma_{su} = 1$, $\xi_3 = 1.45$) led to $S_u = 2614$ kN and $N_u = 2855$ kN. The axial capacity in uplift is therefore

very close to the one in compression, as expected for slender piles in clay. Both capacities within the group were evaluated assuming a group efficiency equal to unity. Figure 11 illustrates the interaction diagrams based on the conventional and the proposed approaches. Both domains were evaluated for two values of the inclination α_M of the applied moment vector M: $\alpha_M = 0$ and $\alpha_M = \pi/n$, with n number of piles supporting a single wind turbine, in order to investigate the effect of the wind direction on the ultimate axial capacity of the foundation. Evidently, the inclination of the resultant moment vector has a negligible effect on both shape and size of the interaction diagrams. This is not surprising, given the small angular spacing among piles.

The design action at foundation level equivalent to extreme wind conditions falls within the conventional domain, in proximity of its boundary. However, the same action is far from the boundary of the domain based on the ultimate capacity of the whole foundation. Hence, there is room for a more rational design.

Different solutions can be investigated by reducing the pile length or the number of piles. Figure 12a shows the interaction diagrams of the whole foundation determined by a progressive reduction of the pile length. For example, the domain with $L = 14$ m, for which piles are still penetrating into the lower stiff clay layer, represents an allowable solution. The total pile length would reduce by about 36% (from 8096 to 5152 m). Similarly, Fig. 12b refers to a foundation layout with 12 piles and different pile lengths; in this case, it would be sufficient to adopt a solution with $L = 19$ m, corresponding to a reduction in the total pile length by 35%. Note that the above domains do not account for the additional strength supplied by yielding moments at the top of piles, which is negligible in comparison with the overall resistance associated with the axial capacity of piles.

6 Conclusions

The common approach employed to assess the bearing capacity of pile groups under vertical eccentric loads assumes as ultimate strength that corresponding to the achievement of the axial capacity on the outermost pile. Such an approach is unduly conservative, since it does not exploit the ductility of the system, and may lead to oversize significantly the pile foundation.

This work suggests an alternative, more rational approach for ultimate moment-axial force interaction diagrams. The problem under examination consists of a rigid cap, clear from the ground, surmounting a group of unevenly distributed, dissimilar piles, each of them having specified values of ultimate load in compression and uplift. The piles' connections to the cap are modeled as either hinges or rigid-plastic fixities. Under the assumption of hinged heads, closed form, exact solutions are provided for the most general case, giving rise to an interaction diagram which is always a convex domain consisting of straight lines and characterized by a point of polar symmetry. For rigid-plastic fixities, a closed-form, lower bound to the collapse load, almost coincident with the exact solution, is provided. Usually, the effect of yielding moment is

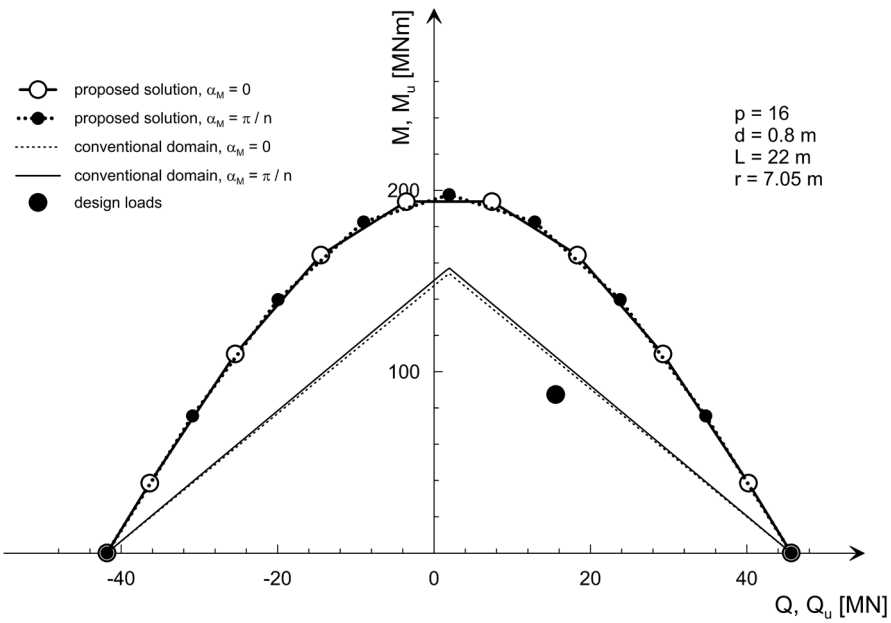

Fig. 11 Design loads, conventional and proposed interaction domains for the foundation of the wind turbine: effect of the moment inclination

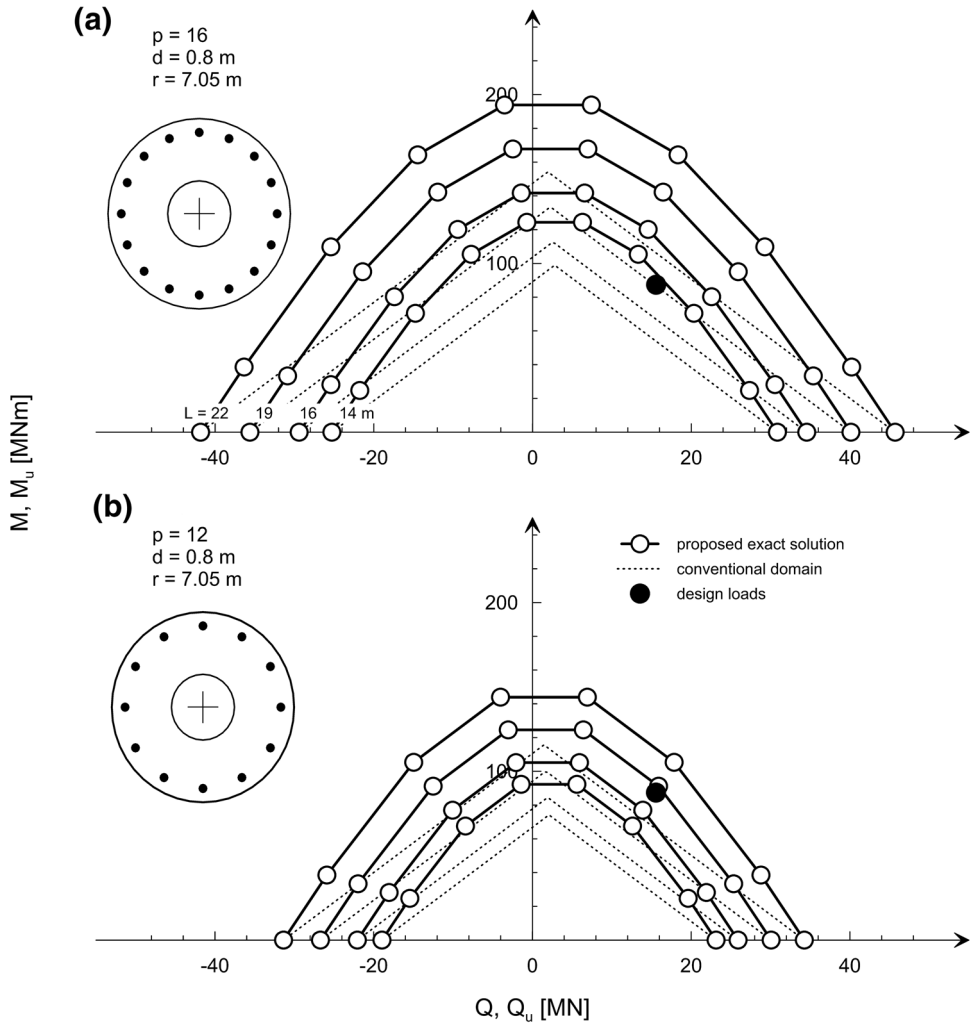

Fig. 12 Effect of the pile length and number on the interaction diagram of the foundation of the wind turbine

negligible for slender piles, while it may be important for large diameter, squatty piles.

With regard to collapse mechanisms, a group of piles loaded eccentrically will fail by a cap rotation about the head of a pile; in this case, all the piles achieve their ultimate axial strength, with the exception of the pile corresponding to the center of rotation. The vertexes of the domain are singularities. If the external load corresponds to a vertex, failure may occur according to a cap rotation about any arbitrary point in between two consecutive piles; in this case, all the piles achieve their ultimate strength.

The proposed approach leads invariably to a more economic ultimate limit state design compared to the common method, regardless of the assumptions made on pile-to-pile interactions effects. An application example to a wind turbine supported by bored piles in stiff clay demonstrates that the proposed approach is very effective in reducing the fondation cost.

It is fair to mention that this work is aimed at providing merely a theoretical framework regarding the bearing capacity of pile groups under vertical eccentric loads. However, it should be kept in mind that the design of such kind of structures is also based on serviceability limit states considerations (i.e., on the evaluation of settlements and rotations and on their comparison with allowable values).

Acknowledgements This research has been developed under the auspices of research projects ReLUIS 2014-2017, granted by Italian Emergency Management Agency.

References

1. AASHTO (2012) AASHTO guide specifications for LRFD seismic bridge design, 2nd edn. American Association of State Highway and Transportation Officials, Washington, D.C.
2. Brand EW, Muktabhant C, Taechathummarak A (1972). Load tests on small foundation in soft clay. In: ASCE conference on

performance of earth and earth supported structures, Purdue University, Indiana, vol. 1, part 2, pp 903–928
3. Briaud JL, Tucker LM, Ng E (1989) Axially loaded 5 pile group and single pile in sand. Proc XII ICSMFE Rio de Janeiro 2:1121–1124
4. Butterfield R, Gottardi G (1994) A complete three dimensional failure envelope for shallow footings on sand. Géotechnique 44(1):181–184
5. CEN (2003) (pr)EN 1997-1. Eurocode 7: geotechnical design—part I: general rules. European Committee for Standardization Technical Committee 250, Brussels, Belgium
6. Cooke RW (1986) Piled raft foundations on stiff clays: a contribution to design philosophy. Géotechnique 36(2):169–203
7. De Mello VFB (1969) Foundations of buildings on clay. State Art Rep Proc VII ICSMFE 1:49–136
8. Dobry R, Gazetas G (1988) Simple method for dynamic stiffness and damping of floating pile groups. Géotechnique 38(4):557–574
9. de Sanctis L, Mandolini A, Russo G, Viggiani C (2002). Some remarks on the optimum design of piled rafts. In: O'Neill & Townsend (eds) ASCE geotechnical special publication 116, Orlando, pp 405–425
10. Fema 750 (2009) Recommended seismic provisions for new buildings and other structures. Building Seismic Safety Council, National Institute of Building, Washington, D.C.
11. Fleming WGK, Weltman AJ, Randolph MF, Elson WK (1992) Piling engineering, 2nd edn. Blackie Academic and Professional, Glasgow
12. Grange S, Kotronis P, Mazars J (2009) A macro-element to simulate dynamic Soil-Structure Interaction. Eng Struct 31(12): 3034–3046
13. Houlsby GT, Cassidy MJ (2002) A plasticity model for the behaviour of footings on sand under combined loading. Géotechnique 52(2):117–129
14. Kezdi A (1957) Bearing capacity of piles and pile groups. In: Proceedings of the IV ICSMFE, London, vol 2
15. Kishida H, Meyerhof GG (1965) Bearing capacity of pile groups under eccentric loads in sand. In: Proceedings of the 6th international conference on soil mechanics, Montreal, Canada, vol 2, pp 270–274
16. Martin CM (2001) Vertical bearing capacity of skirted circular foundations on Tresca soil. In: Proceedings of the 15th ICSMGE, Istanbul, vol 1, pp 743–746
17. Meyerhof GG (1981) The bearing capacity of rigid piles and pile groups under inclined loads in clay. Can Geotech J 18:297–300
18. Meyerhof GG, Ranjan G (1973) The bearing capacity of rigid piles under inclined loads in sand. III: Pile groups. Can Geotech J 10:428–438
19. Meyerhof GG, Yalcin S (1984) Pile capacity for eccentric inclined load in clay. Can Geotech J 21:389–396
20. Meyerhof GG, Yalcin S, Mathur S (1983) Ultimate pile capacity for eccentric inclined load. J Geotech Eng ASCE 109(3):408–423
21. Nova R, Montrasio L (1991) Settlements of shallow foundations on sand. Géotechnique 41(2):243–256
22. NTC (2008). D. M. 14 Gennaio 2008. Norme tecniche per le costruzioni'. Gazzetta Ufficiale della Repubblica Italiana no. 29, 4 Feb 2008 (**in Italian**)
23. O'Neill MW, Hawkins A, Mahar L (1982) Load transfer mechanisms in piles and pile groups. J Geotech Eng Div ASCE 108(GT12):1605–1623
24. Pisanò F, di Prisco C, Lancellotta R (2014) Soil-foundation modelling in laterally loaded historical towers. Géotechnique 64(1):1–15
25. Randolph MF, Jamiolkowski MB, Zdravkovic L (2004). Load carrying capacity of foundations. In: Thomas T (ed) Keynote lecture, proceedings of the Skempton conference 'Advances in Geotechnical Engineering', London, vol 1, pp 207–240
26. Russo G, Viggiani C, de Sanctis L (2004) Piles as settlement reducers: a case history. In: Advances in geotechnical engineering: The Skempton conference: proceedings of a three day conference on advances in geotechnical engineering, organised by the Institution of Civil Engineers and held at the Royal Geographical Society, London, UK, 29–31 March 2004, pp 1143–1154
27. Saffery MR, Tate APK (1961). Model tests on Pile Groups in Clay Soil with particular reference to the behaviour of the group when it is loaded eccentrically. In: Proceedings of the 5th international conference on soil mechanics, Paris, vol 5, pp 129–134
28. Salciarini D, Tamagnini C (2009) A hypoplastic macroelement model for shallow foundations under monotonic and cyclic loads. Acta Geotechnica 4(3):163–176
29. Skempton AW (1951) The bearing capacity of clays. In: Proceedings of building research congress. ICE, London, pp 180–189
30. St John HD, Randolph MF, McAvoy RP, Gallagher KA (1983) The design of piles for tethered platforms. In: Proceedings of the conference on the design and construction of offshore structures. Institution of Civil Engineers, London, pp 53–64
31. Terzaghi K, Peck RB (1948) Soil mechanics in engineering practice. Wiley, New York
32. Vesic AS (1969) Experiments with instrumented pile groups in sand. Performance of deep foundations, vol 444. ASTM Special Technical Publication, West Conshohocken, pp 177–222
33. Viggiani C (1993) Further experience with auger piles in Naples area. In: Inpe WF (ed) Proceedings of the second international geotechnical seminar on deep foundations on bored and auger piles, BAP II. Balkema, Rotterdam, pp 445–458
34. Viggiani C, Mandolini A, Russo G (2011) Piles and piles foundations. Spon Press, London
35. Whitaker T (1957) Experiments with model piles in group. Géotechnique 7(4):147–167